Interaction of Polyphemusin I and Structural Analogs with Bacterial Membranes, Lipopolysaccharide, and Lipid Monolayers†

Lijuan Zhang,‡ Monisha G. Scott,‡ Hong Yan,‡ Lawrence D. Mayer,§ and Robert E. W. Hancock*,‡

Department of Microbiology and Immunology, University of British Columbia, #300-6174 University Boulevard, Vancouver, British Columbia, Canada V6T 1Z3, and BC Cancer Agency, 601 West 10th Avenue, Vancouver, British Columbia, Canada V5Z 1L3

Received May 16, 2000; Revised Manuscript Received September 12, 2000

ABSTRACT: Three structural variants (PV5, PV7, and PV8) of the horseshoe crab cationic antimicrobial peptide polyphemusin I were designed with improved amphipathic profiles. Circular dichroism spectroscopy analysis indicated that in phosphate buffer polyphemusin I, PV7, and PV8 displayed the spectrum of a type II β-turn-rich structure, but, like polyphemusin I, all three variants adopted a typical β-sheet structure in an anionic lipid environment. Both polyphemusin I and variants were potent broad spectrum antimicrobials that were clearly bactericidal at their minimal inhibitory concentrations. The variants were moderately less active in vitro but more effective in animal models. Moreover, these variants exhibited delayed bacterial killing, whereas polyphemusin I killed *Escherichia coli* UB1005 within 5 min at 2.5 μg/mL. All the peptides showed similar abilities to bind to bacterial lipopolysaccharide (LPS) and permeabilize bacterial outer membranes. Consistent with this was the observation that all peptides significantly inhibited cytokine production by LPS-stimulated macrophages and penetrated polyanionic LPS monolayers to similar extents. None of the peptides had affinity for neutral lipids as evident from both tryptophan fluorescence spectroscopy and Langmuir monolayer analysis. As compared to polyphemusin I, all variants showed reduced ability to interact with anionic lipids, and the hemolytic activity of the variants was decreased by 2−4-fold. In contrast, polyphemusin I efficiently depolarized the cytoplasmic membrane of *E. coli*, as assessed using a membrane potential sensitive fluorescent dye 3,3-dipropylthiacarbocyanine ($diSC_3$5) assay, but the variants showed a substantially delayed and decreased depolarizing ability. The coincident assessment of cell viability indicated that depolarization of the bacterial cytoplasmic membrane potential by polyphemusin I occurred prior to lethal damage to cells. Our data suggest that increase of amphipathicity of β-sheet polyphemusin I generally resulted in variants with decreased activity for membranes. Interestingly, all variants showed an improved ability to protect mice both against infection by *Pseudomonas aeruginosa* and from endotoxaemia.

The hemocytes of the horseshoe crab contain a unique family of β-sheet peptide antibiotics, including polyphemusins I and II and tachyplesins I to III (*1*, *2*). These peptides are structurally closely related and are highly abundant in the hemocyte debris. Polyphemusins, isolated from *Limulus polyphemus*, and tachyplesins, isolated from *Tachypleus tridentatus*, *Tachypleus gigas*, and *Carcinoscorpius rotundicauda*, are 18 and 17 residues, respectively. These peptides exhibit a variety of biological activities such as inhibition of the growth of bacteria and fungi and inhibition of the replication of enveloped viruses including vesicular stomatitis virus, influenza A virus, and human immunodeficiency virus (HIV)-1 (*2*−*5*). Other studies indicated that tachyplesin I binds to anionic molecules such as DNA and LPS[1] and inhibits the LPS-mediated activation of factor I, which is an initiation factor in the *Limulus* clotting cascade (*1*, *2*, *6*). Therefore, these arthropod peptides are of special pharmaceutical interest as potential therapeutic agents for anti-endotoxin therapy.

Among the five arthropod peptides, only the secondary structure of tachyplesin I has been determined by nuclear magnetic resonance spectroscopy (*7*). It was found to have a fairly rigid planar conformation consisting of an antiparallel β-sheet structure, constrained by two disulfide bridges and connected by a type II β-turn. In this planar conformation, five bulky hydrophobic side chains are located on one side of the plane, and six cationic side groups are distributed at the "tail" of the molecule. Although the NMR structure was not determined for polyphemusins, they have been proposed to form a similar structure with a similar distribution of positively charged residues due to their extensive sequence identity (*7*). Like many naturally occurring antimicrobial

† This work was supported by the funding of the Canadian Bacterial Disease Network and Canadian Cystic Fibrosis Foundation's SPARx program to R.H. who is also the recipient of a Medical Research Council of Canada Distinguished Scientist Award.

* To whom correspondence should be addressed. Tel: (604) 822−2682, fax: (604) 822−6041, e-mail: bob@cmdr.ubc.ca.

‡ University of British Columbia.

§ BC Cancer Agency.

[1] Abbreviations: CD, circular dichroism; NPN, 1-*N*-phenylnaphthylamine; CCCP, carbonylcyanide-*m*-chlorophenyl hydrazone; CL, cardiolipin; POPC, 1-pamitoyl-2-oleoyl-*sn*-glycero-3-phospho-choline; POPG, 1-palmitoyl-2-oleoyl-*sn*-glycero-3-phosphoglycerol; POPE, 1-pamitoyl-2-oleoyl-*sn*-glycerol-3-ethanolamine; egg-PG, egg-phosphatidyl-DL-glycerol; lysoPG, l-α-lysophosphatidyl-DL-glycerol; lyso-PC, 1-myristoyl-2-hydroxy-*sn*-glycerol-3-phosphocholine; LPS, lipopolysaccharide; MIC, minimal inhibitory concentration.

10.1021/bi0011173 CCC: $19.00 © 2000 American Chemical Society
Published on Web 11/03/2000

peptides, polyphemusins and tachyplesins are polycationic and amphipathic, and the C-terminus is amidated. These properties have been implicated in the mode of action and toxicity of tachyplesin I (*8*). Numerous studies of the antiviral action of this group of peptides against HIV-1 have been carried out (*9*−*11*). However few studies have focused on the antimicrobial mechanism and anti-endotoxin activity. Limited data has indicated that, at high concentrations (>100-fold the inhibitory concentration), tachyplesin I causes morphological and permeability changes of bacterial cells and human erythrocytes and increases the K^+ permeability of *Staphylococcus aureus* and *E. coli* cells, concomitantly reducing cell viability (*12*).

Gram-negative bacteria have two cell envelope membranes. The outer membrane is an asymmetric membrane with the bulky glycolipid lipopolysaccharide (LPS) covering more than 90% of the cell surface in its outer leaflet and phospholipids with a composition similar to that of the cytoplasmic membrane in its inner leaflet. Many antimicrobial cationic peptides have been shown to interact with the LPS of the Gram-negative bacterial outer membrane and pass across this membrane by self-promoted uptake, followed by interaction with and insertion into the negatively charged cytoplasmic membrane (*13, 14*). However, the target of these cationic peptides is not well understood. Although for many peptides the formation of lesions has been observed in model membranes, there has been little convincing evidence to link such interactions to the event(s) causing bacterial cell death, and it has been proposed that at least some peptides cross the cytoplasmic membrane to access cytoplasmic targets such as polyanionic nucleic acids (*15*).

To gain a better understanding of structure−activity relationships and to search for more effective analogues having lower cytotoxicity but adequate or improved antimicrobial and anti-endotoxin activities, we designed and synthesized three derivatives of polyphemusin I. In this study, we investigated the antimicrobial and hemolytic activities of polyphemusin I and its variants and the ability of these variants to bind LPS, to permeabilize the outer and cytoplasmic membranes of Gram-negative bacteria, and to interact with model membrane systems. To acquire information on the lipid specificity of polyphemusin peptides, we have performed surface pressure measurements on monolayers made from LPS as well as charged and uncharged phospholipids. Our results suggest that the modified peptides have improved antimicrobial activities in animal models of infection and endotoxemia, and decreased hemolytic activity was clearly demonstrated. These results also indicate that in vitro antimicrobial activity correlates with the ability of the peptides to interact with anionic phospholipids.

MATERIALS AND METHODS

Strains and Reagents. The bacterial strains used for antimicrobial activity assays included *E. coli* UB1005 (F^-, *nalA37*, *metB1*) and its outer membrane altered mutant DC2 (*16*), *E. coli* KF130 (*gyrA*) (*17*), wild-type strains of *Salmonella typhimurium* (*S. typhimurium*) 14028s (*18*), *S. aureus* ATCC25923 and SAP0017, and the methicillin-resistant *S. aureus* R147. Also included was a clinical isolate of *Staphylococcus epidermidis* (*S. epidermidis*), obtained from Dr. D. Speert, Department of Medicine, University of British Columbia, *Pseudomonas aeruginosa* (*P. aeruginosa*) PAO1 (*19*) and its multidrug resistant mutants H374 (*nalB*) and H744 (*nfxB*) (*20*), and *Enterococcus faecalis* (*E. faecalis*) ATCC 29212. Antifungal activity was tested using a clinical lab isolate of *Candida albicans*. All the strains were grown in Mueller Hinton (MH) broth (Difco Laboratories, Detroit, MI) at 37 °C unless otherwise indicated. The lipopolysaccharides (LPS) of *E. coli* UB1005 and *P. aeruginosa* H103 used for the dansyl-polymyxin B replacement assay were isolated as described by Moore et al. (*21*). Polymyxin B, 1-*N*-phenylnaphthylamine (NPN), carbonyl cyanide-*m*-chlorophenyl hydrazone (CCCP), Re LPS from *Salmonella minnesota* R595 (Re mutant), and LPS from *E. coli* O111:B4 were purchased from Sigma Chemicals Co. (St. Louis, Missouri). Dansyl polymyxin B was synthesized as described previously (*21*). The lipids 1-pamitoyl-2-oleoyl-*sn*-glycero-3-phosphocholine (POPC), 1-palmitoyl-2-oleoyl-*sn*-glycero-3-phosphoglycerol (POPG), 1-palmitoyl-2-oleoyl-*sn*-glycero-3-phospho-ethanolamine (POPE), phosphatidylglycerol from egg yolk (egg-PG), and 1-myristoyl-2-hydroxy-*sn*-glycero-3-phosphocholine (lyso-PC) were purchased from Avanti Polar Lipids Inc. (Alabaster, AL). L-α-Lysophosphatidyl-DL-glycerol (lyso-PG) was purchased from Sigma (St. Louis, Missouri). The fluorescent dye 3,3-dipropylthiacarbocyanine ($diSC_35$) was purchased from Molecular Probes (Eugene, OR).

Peptide Synthesis. All peptides were synthesized by fmoc solid-phase peptide synthesis (*22*) in the carboxyl-terminal amidated form using a model 432A peptide synthesizer (Applied Biosystems Inc, Foster City, CA) at the University of British Columbia Nucleic Acid/Protein service facility. All peptides were oxidized in Tris-DMSO-2-propanol (100 mM Tris-HCl, 25% DMSO, 10% 2-propanol), pH 7.5, for 15−20 h at 23 °C (*23*), to permit formation of disulfide bonds. At the completion of disulfide bond formation, the suspension was loaded onto a reversed-phase FPLC column for purification, resulting in about 20% overall yield. Acid-urea gel analysis showed that the oxidized peptides migrated faster than the corresponding peptides under reducing conditions (in the presence of 2-mercaptoethanol) (data not shown), indicating the presence of a disulfide bridge. MALDI mass spectrometry analysis of the purified peptides indicated the observed molecular mass of the oxidized peptides differed from that of the reduced peptides by four mass units indicating that all four SH groups had covalently bonded, eliminating four H (data not shown). The peptides were apparently homogeneous as judged by their forming a single band on acid urea gels and a single peak on reverse phase FPLC (data not shown).

Circular Dichroism (CD) Spectroscopy. CD spectra were recorded on a model J-810 spectropolarimeter (Jasco, Tokyo, Japan) connected to a Jasco spectra manager, using a quartz cell of 1-mm path length. CD spectra were measured, at 25 °C, between 190 and 250 nm at a scanning speed of 10 nm/min in 10mM sodium phosphate buffer, pH 7.2, in the presence or absence of 10 mM lyso-PC/lyso-PG (1:1). Minor contributions of circular differential scattering were eliminated by subtracting the CD spectrum of buffer and lyso-PC/lyso-PG alone from that of peptide in buffer and lyso-PC/lyso-PG, respectively. The spectra shown are the averages of 10 scans.

Minimal Inhibitory Concentration Assay (MIC). The peptide MIC for a range of microorganisms was determined by the modified broth microdilution method in Muller Hinton (MH) medium using polypropylene microtiter plates (*24*). The MIC was determined as the lowest peptide concentration at which growth was inhibited after overnight incubation of the plates at 37 °C. MICs were performed three times on different occasions, and the median values are shown. Killing assays were performed at 2.5 μg/mL of each peptide (about 10−20-fold MIC). Cells were plated on MH agar plates after defined time intervals and incubated at 37 °C overnight, and colony-forming units were counted.

Hemolytic Assay. The hemolytic activity of the peptides was tested against human red blood cells as described previously (*25*).

Anti-Endotoxin Assay. The anti-endotoxic activity of the peptides was tested in an in vitro assay as described previously (*26*). Briefly, the murine macrophage cell line RAW 264.7 was obtained from American Type Culture Collection (Manassas, VA) and grown in DMEM medium supplemented with 10% fetal calf serum. The cells were plated at a density of 10^6 cells/well in 24-well plates, incubated overnight, and then washed with fresh medium. The cells were stimulated for 6 h with 100 ng/mL *E. coli* O111:B4 with and without 20 μg/mL. The cell supernatants were assayed for TNF-α and IL-6 by enzyme-linked immunosorbent assays (ELISA) (Endogen, Hornby, ON, Canada), following the manufacturer's suggestions.

Animal Models. To measure the protective activity of the peptides against mice challenged with *P. aeruginosa*, a 100% lethal dose of *P. aeruginosa* M2 (approximately 200 organisms) was injected intraperitoneally into female CD-1 mice that had been made neutropenic by three injections of cyclophosphamide (*26*). Then 100 μL of sterile water containing 200 μg of peptide was injected after 30 min into the peritoneum of groups of five mice. Survival was recorded from 24 to 72 h, after which no further mice died.

To test the anti-endotoxic activity of peptides, endotoxic shock was induced by intraperitoneal injection of 100 μL of 3 μg/mL of *E. coli* O111:B4 LPS in phosphate-buffered saline (PBS, pH 7.2) into galactosamine-sensitized 8−10-week-old female CD-1 mice (*23*). Peptide (200 μg in sterile water) was injected intraperitoneally at a separate site within 10 min of LPS injection, and survival was monitored up to 24 h postinjection after which no further mice died.

Dansyl Polymyxin B Displacement Assay. The relative binding affinity of each peptide for LPS was determined using the dansyl polymyxin B displacement assay of Moore et al. (*21*), using LPS isolated from *E. coli* UB1005. Maximal displacement of LPS was expressed as a percentage in which 100% displacement of dansyl polymyxin B was taken as that observed with polymyxin B.

Membrane Permeabilization Assay. The outer membrane permeabilization activity of the peptide variants was determined by the 1-*N*-phenylnaphthylamine (NPN) uptake assay of Loh et al. (*27*), using intact cells of *E. coli* UB1005. The concentration of peptide leading to a 50% of maximal increase in NPN uptake was recorded as the P_{50}.

The cytoplasmic membrane depolarization activity of the peptides was determined (*24*) using the membrane potential sensitive dye 3,3-dipropylthiacarbocyanine ($diSC_3$5) (*28*) and *E. coli* DC2. Bacterial cells in mid-log phase were centrifuged, washed in 5 mM HEPES, pH 7.8, and resuspended in the same buffer to an OD_{600} of 0.05. A stock solution of $diSC_3$5 was added to a final concentration of 0.4 μM and quenching was allowed to occur at room temperature for 20−30 min. Then KCl was added to the cell suspension to final concentration of 100 mM to equilibrate the cytoplasmic and external K^+ concentrations. A 2-mL cell suspension was placed in a 1-cm cuvette, and the desired concentration of tested peptide was added. Changes in fluorescence due to the disruption of the membrane potential ($\Delta\psi$) in the cytoplasmic membrane were continuously recorded using a Perkin-Elmer model 650-10S spectrofluorimeter at an excitation wavelength of 622 nm and an emission wavelength of 670 nm. Control experiments employing valinomycin and varying concentrations of K^+ demonstrated that the increase in $diSC_3$5 fluorescence was inversely proportional to the residual $\Delta\psi$ (*24*).

In some experiments, the residual cell viability was assessed alongside the $diSC_3$5 assay. Briefly, cells were prepared as described above and resuspended in 5 mM HEPES (*N*-2-hydroxyethylpiperazone-*N*′-2-ethane sulfonic acid), pH 7.5, 5 mM glucose, 0.4 μM $DiSC_3$5, and 150 mM KCl. The cell suspension was incubated at room temperature until dye uptake was maximal. Then a 2-mL cell suspension was placed in a 1-cm cuvette, and the desired concentration of the tested peptide was added. Changes in fluorescence intensity due to disruption of the membrane potential were recorded, and at regular intervals, the surviving cells were plated on MH agar plates and incubated at 37 °C overnight to assess residual colony forming units.

Peptide Interaction with Model Membrane Systems. Unilamellar liposomes (0.1 μm) in HEPES buffer, pH 7.5, were prepared with POPC/POPG (7:3 w/w) or POPC only, using the freeze−thaw method as described previously (*29*) followed by extrusion through 0.1-μm double-stacked Nuclepore filters using an extruder device (Lipex Biomembranes, Vancouver, BC, Canada). The tryptophan fluorescence and KI quenching measurements were performed using a Luminescence spectrometer, LS50B (Perkin-Elmer) as described previously (*30*).

Langmuir Monolayer Assay. Lipid monolayers were formed by applying the appropriate lipids dissolved in hexane or chloroform onto water contained in a circular Teflon trough ($d = 4.5$ cm, total volume of 11.5 mL). Monolayers were allowed to equilibrate until a stable surface pressure was obtained (<0.2 mN/m drift in surface pressure $\Delta\pi$). A small port in the side of the trough enabled injection of reagents into the subphase without disruption of the monolayer. The subphase was gently mixed with a magnetic stir bar at 45 rpm. Surface pressure measurements were obtained by using the Whilhelmy plate method (*29*). The plate was cleaned with methanol three times and thoroughly rinsed with double-distilled water prior to each surface pressure measurement. The experiments were run at 23 °C.

An LPS monolayer film on the air−water interface was obtained by spreading the LPS solution (0.5 mg/mL in chloroform/methanol/H_2O, 17/7/1, v/v) (*32*) onto buffer alone (5 mM HEPES and 150 mM NaCl) or in the presence of either 2 mM or 5 mM $MgCl_2$.

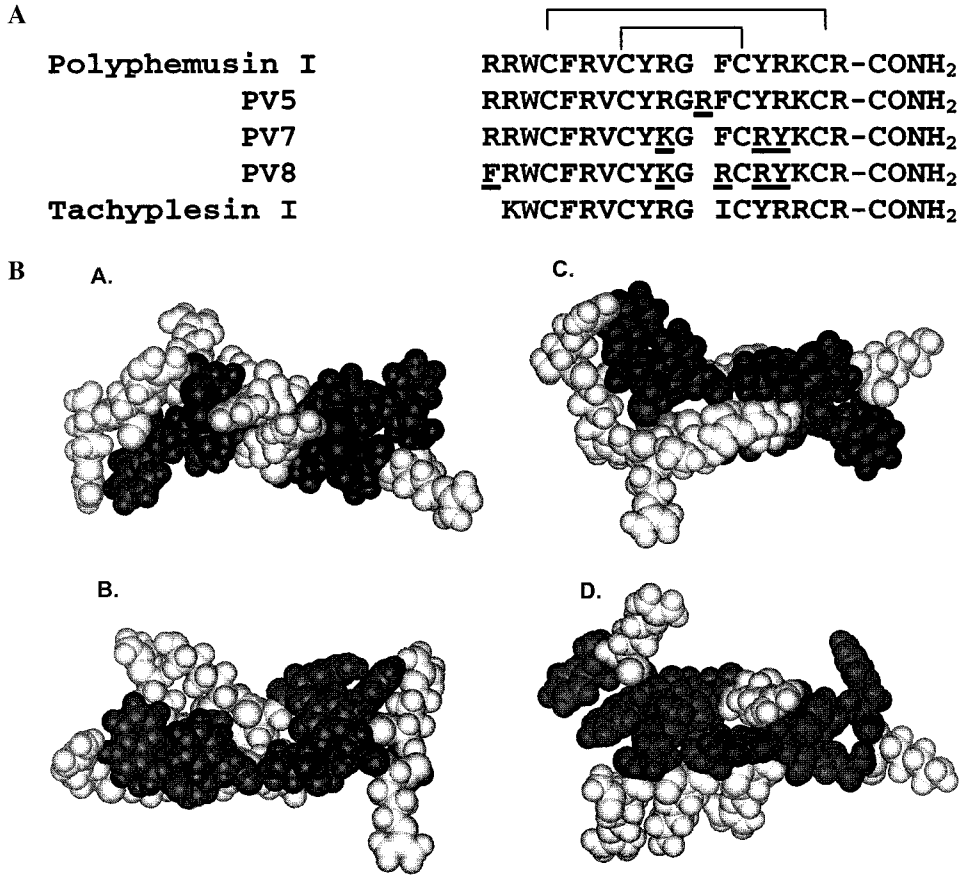

FIGURE 1: (A) Amino acid sequence (one letter amino acid code) of tachyplesin, polyphemusin I and its variants. Disulfide linkages are shown by solid lines. The amino acids substituted in the variants are underlined. (B) Model structure of polyphemusin I and variants predicted by Insight II peptide modeling program (Biosym Inc., San Diego, CA). Dark color indicates apolar residues and light color indicates charged residues. A. Polyphemusin I; B. PV5; C. PV7; D. PV8.

RESULTS

Design and Structure Determination of the Polyphemusin Variants. The amino acid sequence of polyphemusin I and its structural analogues is shown in Figure 1, panel A. The structure is assumed to be a double-stranded β-sheet, stabilized by two disulfide bonds based on their CD spectrum and homology with tachyplesin I (*7*). The two β-strands are connected by a β-turn. The purpose of the structural variations was to increase the segregation of charged and hydrophobic residues (amphipathicity). Among the three variants synthesized, the closest structural analogue to polyphemusin I was PV7 in which a positional switch was made between R_{14} and Y_{15}, in addition to a conservative substitution at position 10 ($R_{10} \rightarrow K_{10}$). PV5 was a variant with an additional arginine residue inserted between G_{11} and F_{12} in the loop region. This would not only increase the total positive charge of the peptide but also the size of the loop. In PV8, the residues at positions 1 and 12 were switched ($F_{12} \rightarrow R_{12}$, $R_1 \rightarrow F_1$) increasing the net positive charge and hydrophilicity of the loop and altering the tail region to decrease flexibility and hydrophobicity due to the hydrophobic nature and bulky aromatic ring of phenylalanine.

In general, all three variants were predicted to have increased amphipathicity as compared to polyphemusin I as judged from molecular modeling using the Insight II protein-peptide modeling program (Figure 1, panel B). In addition, the variants had altered loop regions that were predicted to be more hydrophilic and in one case, PV5, larger.

Circular dichroism (CD) spectroscopy was carried out for all the peptides included in this study. The CD spectrum of polyphemusin I in aqueous buffer displayed two positive bands at about 224 and 202 nm (Figure 2), a spectrum typical of a structure dominated by a type II β-turn and virtually identical to the published CD spectrum for tachyplesin I (*33*). It is worthwhile to note that aromatic amino acids have been suggested to partially contribute to the 224 nm band (*34*). We utilized 10 mM lyso-PC/lyso-PG (1:1) as an anionic membrane-mimicking environment. Under this condition, polyphemusin I exhibited positive ellipticity maxima near 230 and below 200 nm and a negative ellipticity around 205 nm (Figure 2), indicating a typical β-sheet structure and virtually identical to the CD spectrum of tachyplesin I in acidic liposomes (*31*). Tachyplesin and polyphemusin are highly related to one another (Figure 1, panel A). Therefore, the secondary structure of polyphemusin I is very likely to be similar to that of tachyplesin I with an antiparallel β-sheet structure stabilized by disulfide bridges and a type II β-turn. The three variants revealed fundamentally similar spectra in the presence of lyso-PC/lyso-PG (1:1) having positive ellipticities near 230 nm and below 200 nm and a negative ellipticity near 205 nm, indicating they have almost the same backbone conformations as polyphemusin I (Figure 2). In phosphate buffer, the CD spectra for the three variants were generally similar in shape to that of polyphemusin I, but the intensities of positive ellipticities and wavelengths were slightly different from one another, which was more apparent

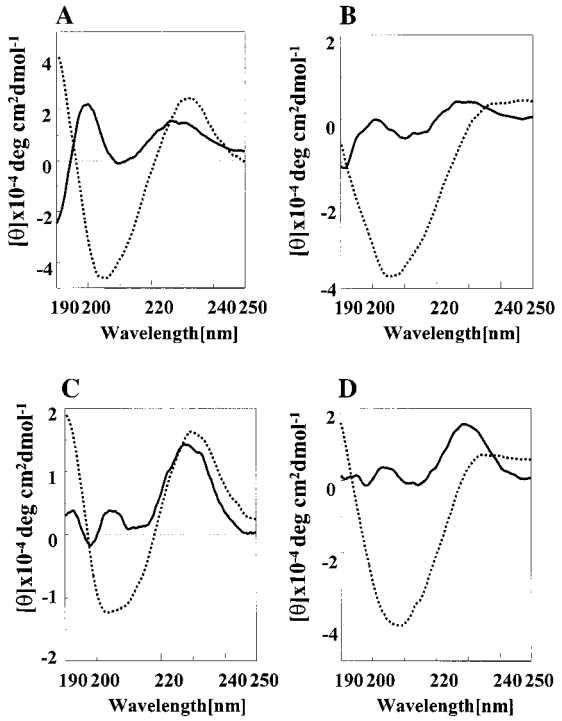

FIGURE 2: Circular dichroism spectra of (A) polyphemusin I; (B) PV5; (C) PV7; and (D). PV8 in phosphate buffer (solid lines) and in 10 mM lyso-PC/lysoPG (1:1) (dotted lines). Peptides were used at a concentration of 25 μM.

for PV5. However, such moderate changes in wavelength and in the magnitude of maximum or minimum ellipticities without altering major backbone structure have been published for tachyplesin analogues due to amino acid substitutions in the peptide (*31*). Possibly, the variants displayed a less pronounced β-turn in phosphate buffer due to the residue changes induced in this region, although similar β-sheet structure was evident in lyso-PC/lyso-PG (1:1). This suggests that mispairing among the four-cysteine residues is very unlikely, since this would abolish type II β-turn and β-sheet structure, as predicted by the Insight II modeling program (data not shown). Nevertheless, it is worth noting that the precise structure of the variants, especially PV5, needs to be verified using more sophisticated techniques such as two-dimensional NMR methods.

Antimicrobial and Hemolytic Activities. The minimal inhibitory concentrations (MIC) of each peptide for a panel of microorganisms is shown in Table 1. These were the most active peptides we have ever worked with. Polyphemusin I showed high antimicrobial activity against both Gram-negative and Gram-positive bacteria with MICs ranging from 0.125 to 0.5 μg/mL. It was highly active against the yeast *C. albicans* with an MIC of 1 μg/mL. Polyphemusin I was also quite hemolytic, and the concentration required to lyse human red blood cells was around 20 μg/mL (Table 1). As compared to polyphemusin I, the variants were slightly less active for most bacteria and had MICs that were 1−2-fold higher than those of the parent peptide (Table 1). However, for the Gram-negative bacterium *P. aeruginosa* and the yeast *C. albicans* somewhat larger differences were observed for PV7 (2−4-fold) and PV8 (8−16-fold).

The MICs and minimal bactericidal concentrations were in all tested cases identical, suggesting that these peptides were bactericidal in nature. To confirm this we performed

Table 1: Antimicrobial (MIC) and Hemolytic Activities of Peptide Variants against Bacteria, Fungus, and Human Red Blood Cells (hRBC)

	MIC (μg/mL)			
cells	PMI[a]	PV5	PV7	PV8
E. coli UB1005	0.125	0.25	0.25	0.25
E. coli DC2	0.125	0.25	0.125	0.25
E. coli KF130	0.125	0.25	0.125	0.25
S. typhimurium 14028s	0.25	0.5	0.5	0.5
P. aeruginosa PAO1	0.25	1	1	2
P. aeruginosa H374	0.25	0.5	0.5	2
P. aeruginosa H744	0.25	1	1	2
S. aureus ATCC 25923	0.5	1	1	1
S. aureus R147	0.5	1	1	1
S. aureus SAP0017	0.5	1	1	1
S. epidermidis	0.25	0.25	0.5	0.5
E. faecaelis	0.25	0.5	0.25	0.5
C. albicans	1	2	4	16
human red blood cells[b]	21.3	42.6	85	85

[a] Polyphemusin I. [b] This row represents the hemolytic activity of the peptide expressed as the minimal concentration of peptide (in μg/mL) resulting in complete lysis of human red blood cells.

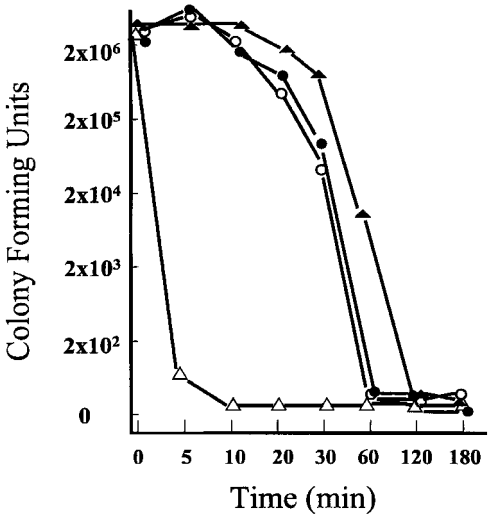

FIGURE 3: Killing kinetics of polyphemusin I and its variants against *E. coli* UB1005. △, polyphemusin I; ●, PV5; ○, PV7; and ▲, PV8 at 2.5 μg/mL.

killing assays against *E. coli* UB1005 at a concentration of 2.5 μg/mL. Polyphemusin I exhibited very rapid killing, and no cells could form colonies after 5 min of treatment. However, the variant peptides demonstrated no killing for 20−30 min, and 100% cell killing only occurred after 1 h (2 h in the case of PV8), indicating they lead to delayed cell killing (Figure 3).

The hemolytic activity of the variants was also decreased, and the concentration required to lyse human red blood cells was from 2- to 4-fold higher (Table 1). Overall, the therapeutic indices (concentration required to lyse red blood cells divided by the concentration required to kill bacteria) were quite similar, ranging from 42 to 680 for the different peptides and bacteria.

LPS Binding Affinity. A variety of cationic antimicrobial peptides have been shown to interact with the LPS of the Gram-negative bacterial outer membrane, permeabilize the outer membrane, and then pass across this membrane by a process termed self-promoted uptake (*24*−*26*). To assess the binding of peptides to bacterial LPS, we examined the ability

Table 2: Ability of Peptides to Bind to *E. coli* LPS as Judged by the Dansyl Polymyxin Displacement Assay and Ability to Permeabilize and Promote NPN Uptake Across Outer Membrane of *E. coli* Ub1005

peptide	I_{50} (μM)[a]	I_{max} (%)[b]	P_{50} (μg/mL)[c]
polyphemusin I	4.8	85	2.8
PV5	3.0	87	3.7
PV7	5.7	76	4.1
PV8	4.9	93	3.9
polymyxin B	5.6	100	ND

[a] Concentration leading to half-maximal DPX displacement. [b] Maximal DPX displacement relative to polymyxin B. [c] Concentration leading to half-maximal NPN uptake.

of each peptide to displace LPS-bound dansyl polymyxin, a cationic probe that is highly fluorescent only when bound (Table 2). The fraction of dansyl polymyxin B remaining bound to LPS was plotted as a function of peptide concentration. Using this plot, the concentration of each peptide required to reduce the amount of bound dansyl polymyxin B (10 μM) by 50% of the maximal displacement (I_{50}) was determined (Table 2). All peptides displaced dansyl polymyxin to similar extent with I_{50} values that differed by less than 2-fold (Table 4), with PV5 demonstrating the best binding to LPS.

Membrane Permeabilization Activity. The ability of the peptides to permeabilize the outer membrane of *E. coli* UB1005 is shown in Table 2. NPN is a small hydrophobic molecule that is normally excluded by the intact outer membrane but exhibits increased fluorescence when it partitions into the bacterial outer membrane after disruption of outer membrane integrity. Therefore, an increase in fluorescence in the presence of a peptide indicates the ability of peptide to permeabilize the bacterial outer membrane. As shown in Table 2, both polyphemusin I and its variants were able to mediate NPN uptake across the outer membrane to similar extents, and the concentration for half-maximal NPN uptake (P_{50}) varied less than 30% from a mean of 3.6 μg/mL.

After passage through the outer membranes of Gram-negative bacteria, or through the permeable cell walls of Gram-positive bacteria, cationic antimicrobial peptides interact with the bacterial cytoplasmic membrane. Bacteria normally maintain a membrane potential gradient ($\Delta\psi$) of around −140 mV at neutral pH. This can be assessed using the membrane potential sensitive dye $diSC_35$ that is taken up by energized cells according to $\Delta\psi$ and concentrates in the cell membrane leading to quenching of $diSC_35$ fluorescence (*24*). The ability of each peptide to depolarize the *E. coli* cytoplasmic membrane potential gradient resulting in a loss of $diSC_35$ from cells into the buffer, and a corresponding increase in fluorescence can be measured. In this study, the kinetics of depolarization of membrane potential by the peptides was assessed coincident with measurement of cell viability over a 1-h time period (Figure 4). Polyphemusin I was a relatively good membrane permeabilizer and, at a concentration of 0.2 μg/mL (twice the MIC), caused rapid dissipation of the cytoplasmic membrane potential over the first 2 min without any lag time. The maximal dye release was reached within 10 min (Figure 4). Assessment of cell viability indicated that there was less than a one log decrease in colony forming units up to 30 min of membrane permeabilization and only a 2-log decrease in colony forming units was observed up to 60 min, indicating that dissipation of cytoplasmic membrane potential occurred prior to cell killing as assessed by the reduction in colony forming bacteria. In contrast, at the same peptide concentration, both PV7 and PV8 caused significantly slower membrane permeabilization, with a lag time of more than 10 min before substantial fluorescence increase was detected (Figure 4) and a maximum dye release that was less than 50% of that mediated by polyphemusin I. At a concentration of 0.2 μg/mL, PV5, PV7, and PV8 caused dye release from the cytoplasm at only 5%, 20%, and 23% of the rate mediated by polyphemusin I addition. Cell viability test indicated that there was very little change in numbers of colony forming bacteria after treatment of the cells with the three variants during the 60 min of the membrane permeabilization assay.

Interaction of Peptides with Liposomes. Because of these obvious differences in interaction of these peptides with the bacterial cytoplasmic membrane, we turned to model systems in an attempt to explain the results. The tryptophan residue at position 3 of the polyphemusin peptides provided the possibility to monitor binding to liposomes since the fluorescence emission of this amino acid is sensitive to the polarity of its environment. Upon addition of each peptide to anionic liposomes with a composition that reflected the uncharged to charged phospholipid ratio of the *E. coli* cytoplasmic membrane (POPC/POPG, 7:3), the fluorescence emission maxima exhibited a blue shift of 11 to 14 nm and marked increase in fluorescence emission intensity (1.3−3.7-fold), indicating a relocation of this tryptophan residue into a more hydrophobic environment (Table 3). No significant differences were observed among these peptides. To confirm this conclusion, we looked at the ability of the water-soluble quencher KI to suppress peptide tryptophan fluorescence. In buffer, the water-soluble quencher KI was able to completely suppress fluorescence in a concentration-dependent manner (Figure 5). However, when the quencher was added to peptide in the presence of liposomes (POPC/POPG, 7:3), the fluorescence intensity remained essentially unchanged, indicating that the tryptophan residue of the peptides in liposomes was inaccessible to this aqueous quencher (Figure 5). The addition of peptide to uncharged POPC liposomes did not result in a significant blue shift (generally less than 2 nm), and the tryptophan fluorescence of three of the peptides decreased, whereas that of PV7 increased about 50% in POPC liposomes as compared to HEPES buffer (Table 3). Addition of the quencher KI to peptide in the presence of POPC liposomes resulted in suppression of tryptophan fluorescence in a concentration-dependent manner similar to peptide in buffer (Table 3), suggesting that the tryptophan residue of the polyphemusin peptides in the presence of POPC liposomes was still accessible to the quencher. Thus, the changes in intensity of tryptophan fluorescence in the presence of POPC may reflect light scattering by the liposomes and/or association of the peptides with the surfaces of liposomes.

Interaction of Peptides with Lipid Monolayers. Lipid monolayers at an air/water interface provide a simple, sensitive model for mimicking biological membranes, and many studies have shown that the monolayer technique is a powerful tool to assess membrane insertion of proteins and peptides.

Table 3: Tryptophan Fluorescence Emission Maxima (E_{max}) of Polyphemusin I and Variants in HEPES Buffer or in the Presence of POPC/POPG (7:3) Liposomes or POPC Liposomes

peptide	E_{max} (nm) in HEPES buffer	E_{max} (nm) in POPC/POPG	intensity change (F/F_0)	accessibility to quencher KI[b]	E_{max} in POPC (nm)	intensity change (F/F_0)	accessibility to quencher KI[b]
PMI[a]	356	342	1.3	−	353	−0.5	+
PV5	356	342	3.7	−	354	−0.7	+
PV7	354	343	2.4	−	353	1.5	+
PV8	353	338	1.9	−	350	−0.7	+

[a] Polyphemusin I. [b] (−) the fluorescence of tryptophan residue could not be quenched by the aqueous quencher KI; (+) the fluorescence of tryptophan residue was suppressed by the aqueous quencher KI in a concentration-dependent manner.

Table 4: Peptide-Mediated Inhibition of TNF-α and IL-6 Production by RAW Macrophages Stimulated with O111:B4 LPS (100 ng/mL)

peptide treatment (20 μg/mL)	inhibition of TNF-α (%)	inhibition of IL-6 (%)
polyphemusin I	83 ± 6	84 ± 3
PV5	90 ± 6	91 ± 4
PV7	61 ± 5	77 ± 6
PV8	55 ± 5	70 ± 6

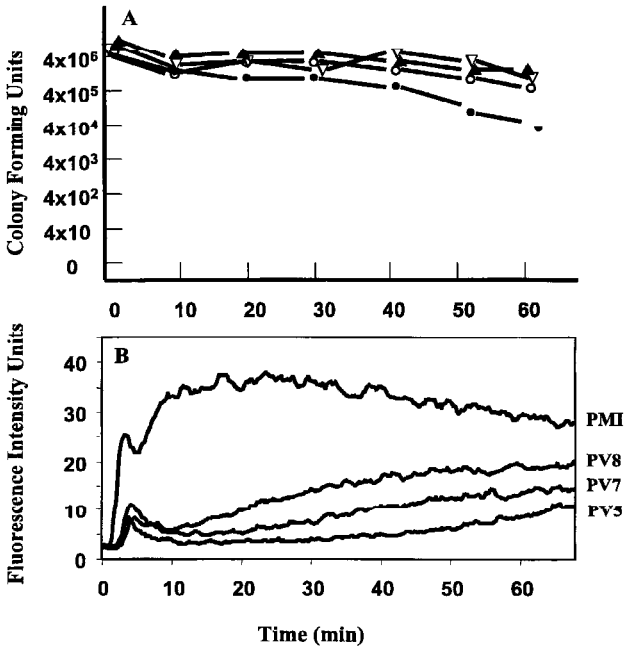

FIGURE 4: (A) Cell viability measurement during cytoplasmic membrane depolarization of *E. coli* DC2 as assessed by the $diSC_35$ assay at 0.2 μg/mL of each peptide. ●, polyphemusin I; ▽, PV5; ○ PV7; ▲, PV8. (B) Kinetics of cytoplasmic membrane depolarization under the same condition and same peptide concentration as in cell viability test in panel A.

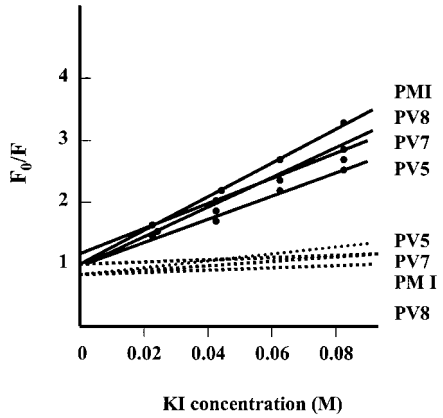

FIGURE 5: Stern−Volmer plot of the quenching of peptide trypophan fluorescence by the aqueous quencher KI. Dotted lines represent data for peptides incorporated into a suspension of liposomes (POPC/POPG, 7:3), while solid lines represent data for quenching in 10 mM HEPES buffer, pH 7.5.

The primary phospholipids of *E. coli* cells comprise a mixture of the neutral lipid phosphatidyl ethanolamine (PE) and the anionic lipids phosphatidyl glycerol (PG) and cardiolipin (CL), in the ratio of 78:4.7:14.4 (*35*). In addition, various minor lipid species are also found (*35*). We prepared monolayers from POPE/egg-PG/CL (78:4.7:14.4) to mimic the *E. coli* cytoplasmic membrane and tested the ability of polyphemusin peptides to interact with such monolayers. Molecules that interact only with the headgroups of monolayer lipids typically induce minimal changes in surface pressure. In contrast, insertion into the hydrophobic region of the lipid monolayer can cause a significant increase in monolayer surface pressure. Thus, when a protein or peptide molecule is injected into the subphase bathing a monolayer, the degree of surface pressure change ($\Delta\pi$) can be used to resolve whether peptide−membrane interactions include insertion and disturbance of the fatty acyl core of the membrane. Figure 6, panel A, shows the variation in surface pressure as a function of peptide concentration. The degree of surface pressure change induced by peptides ($\Delta\pi_{max}$ 4.5−7.4 mN/m) with negatively charged monolayers was consistent with penetration of the peptides into the hydrophobic portion of the monolayer since surface interactions typically are reflected by $\Delta\pi$ values < 2 mN/m (*31*). All peptides induced increases in surface pressure that were a sigmoidal function of peptide concentration (Figure 6, panel A), a result consistent with a cooperative interaction of the peptide molecules with a monolayer. Consistent with its superior ability to depolarize the bacterial cytoplasmic membrane, polyphemusin I was the most effective peptide at modulating the surface pressure as indicated by the plateau $\Delta\pi$ values, which were 7.4, 5.2, 4.7, and 4.5 mN/m for polyphemusin I, PV5, PV7, and PV8, respectively.

The lipid specificity of each peptide was monitored by the extent of the surface pressure change upon addition of 1 μg/mL of peptide to the subphase of monolayers of POPC, POPE, egg-PG, or CL (Figure 6, panel B). All peptides selectively interacted with negatively charged lipids and generally had a greater effect on PG than on CL monolayers. Consistent with the observations in Figure 6, panel A, polyphemusin I demonstrated the largest effect on PG monolayers. None of the peptides were able to penetrate monolayers composed of neutral lipids such as POPC or POPE.

To mimic interactions with the outer membrane, monolayers prepared with LPS were employed to mimic the outer

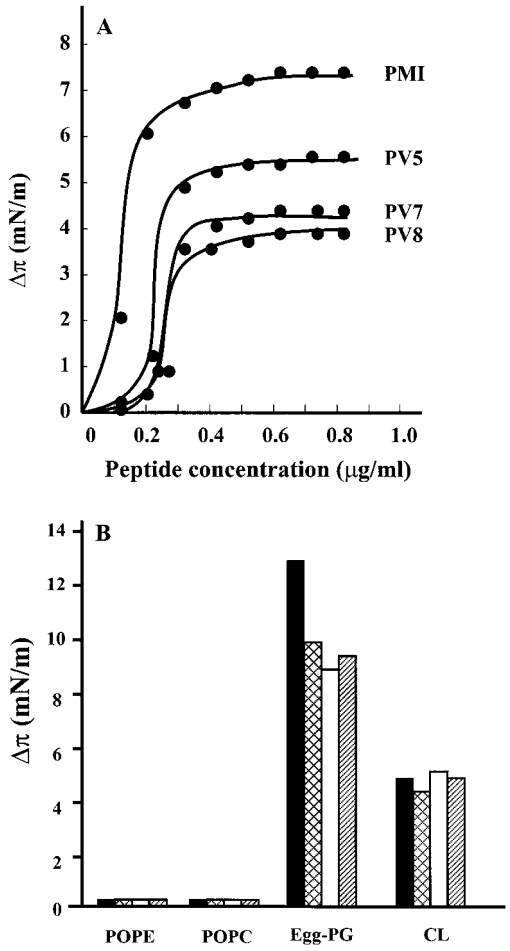

FIGURE 6: Influence of peptide addition to the aqueous subphase bathing lipid monolayers, on the surface pressure as measured in a Langmuir balance. (A) Plot of the surface pressure increase as a function of peptide concentration. Monolayers were spread with mixed lipids (POPC/egg-PG/CL in a ratio of 78:4.7:14.7, v/v), creating an initial pressure of 20 ± 1 mN/m and allowed to stabilize for 5 min before peptide addition. Titration of the surface pressure increase was accomplished by adding successive amounts of peptide to the subphase while continuously monitoring the surface pressure of the film. (B) Influence on surface pressure of the addition of 1 μg/mL peptides to the aqueous subphase bathing monolayers made from either POPC, POPE, egg-PG, or CL. Solid bars, polyphemusin I; crosshatched bars, PV5; unfilled bars, PV7; hatched bars, PV8. The results shown are the averages of two independent experiments.

leaflet of Gram-negative bacterial outer membrane. Thus the ability of a peptide to interact with an LPS monolayer may be expected to reflect its ability to penetrate the outer membrane. As shown in Figure 7, no substantial differences were observed between polyphemusin I and its variants in terms of their ability to interact with LPS monolayers. These peptides demonstrated similar abilities to penetrate LPS monolayers in the absence of added Mg^{2+}. Consistent with the observation that peptides generally interact with divalent cation binding sites on LPS, the addition of Mg^{2+} resulted in a concentration dependent, moderate reduction in peptide-mediated surface pressure change (Figure 7).

Anti-Endotoxic Activities in RAW 264.7 Macrophages. Since all of the polyphemusins bound to *E. coli* LPS, the peptides were tested for their ability to inhibit *E. coli* O111:B4 LPS induced production of TNF-α and IL-6 in RAW macrophages. The peptides, at 20 μg/mL, were all able to significantly inhibit cytokine production by LPS-stimulated

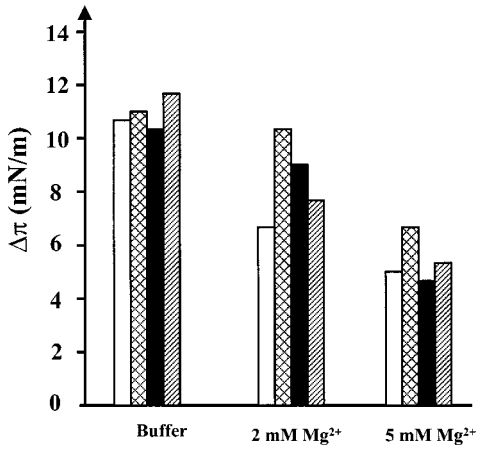

FIGURE 7: Influence on surface pressure of the addition of 0.8 μg/mL peptide to the aqueous subphase bathing *S. minnesota* Re LPS monolayers. The Mg^{2+} concentration of the subphase was varied. The monolayer was spread achieving an initial pressure of 18 ± 1 mN/m and allowed to stabilize for 5 min before addition of peptide. Unfilled bars, polyphemusin I; crosshatched bars, PV5; solid bars, PV7; hatched bars, PV8.

Table 5: Peptide-Mediated Protection in Mice after Intraperitoneal Challenge with Bacteria or LPS Followed by a Single Intraperitoneal Injection of 200 μg of Peptide Per Mouse after 30 min

peptide treatment	*P. aeruginosa* infection in neutropenic mice[a]		endotoxemia in galactosamine-sensitized mice[b]
	mean time to death (h)	survival (%)	survival (%)
none	24	0	0
PMI[c]	52	20	10
PV5	57	40	50
PV7	61	40	40
PV8	>72	60	20

[a] Groups of 5 mice. [b] Groups of 10 mice. [c] Polyphemusin I.

macrophages (Table 4). PV5, which demonstrated the best binding to LPS (Table 4), was the best inhibitor of TNF-α and IL-6 followed by polyphemusin I and the other peptides (Table 4). The peptides were also able to inhibit LPS-LBP (LPS binding protein) interaction in an LBP ELISA-like assay, with PV5 being the best inhibitor (data not shown).

Anti-infection and anti-endotoxic activities in animal models. The ability of the peptides to protect against a *P. aeruginosa* M2 infection in the neutropenic mouse model is shown in Table 5. Mice that received no peptides died rapidly after bacterial challenge, resulting in 50% of mortality in 24 h and 100% mortality in 41 h, while 100% of control, unchallenged mice survived during the observation period (Table 5). All peptides given as a single dose of 200 μg per mouse 30 min after the bacterial challenge, were able to provide some degree of protection with more than 50% of mice surviving after 48 h of bacterial challenge. However, although it had the best in vitro antimicrobial activity against *P. aeruginosa*, polyphemusin I showed relatively poor protective activity as judged by survival and mean time to death. The variants, on the other hand, showed higher protective activity in mice against challenges with *P. aeruginosa* M2 despite their obviously increased MICs for *P. aeruginosa*. This indicates that there are other factors in in vivo protectiveness than simple antibacterial activity, e.g.,

in vivo stability, anti-endotoxic activity, or synergy with other factors such as lysozyme that exist in vivo.

Bacterial endotoxin (LPS) is highly toxic and can cause high mortality in both humans and animals when released during Gram-negative bacterial infection. Galactosamine-treated mice given moderate doses of endotoxin usually die from endotoxic shock within 17 h. Again polyphemusin I did not seem to be highly protective against endotoxic shock in this mouse model, but all three variants provided higher protection in mice against endotoxin-induced death with PV5 being the best of the three (Table 5).

DISCUSSION

Natural antimicrobial cationic peptides can adopt many different secondary structures including amphipathic α-helices such as cecropins, extended structures such as indolicidin, β-sheets such as the defensins, and loops such as bactenecin (*36*−*39*). We have been studying all of these classes, including improved synthetic variants, and in our experience, polyphemusin I is the most active cationic bactericidal peptide isolated to date. It had in vitro MICs ranging from 0.125 to 0.5 μg/mL against bacteria and a MIC of 1 μg/mL against the yeast *C. albicans* (Table 1). We designed three structural analogues by increasing the amphipathicity of polyphemusin I to search for potent variants. We demonstrate here that these variants are novel peptides with interesting in vitro activities (albeit in some cases, slightly weaker than those of polyphemusin I but superior to most other antimicrobial peptides) but with decreased hemolytic activity and more importantly with improved protective activity in vivo against *P. aeruginosa* infection and against endotoxic shock.

Both polyphemusin I and its variant peptides tended to interact selectively with negatively charged phospholipids as evidenced by both tryptophan fluorescence spectroscopy and phospholipid monolayer studies. The lack of affinity of these peptides for neutral lipids is in agreement with the early findings that the analogue peptide, tachyplesin I, decreased the phase-transition temperature of an artificial membrane composed of dipalmitoylphosphatidylglycerol but did not affect that of a dipalmitolyphosphatidylcholine membrane (*12*). The reduced affinity of the variants for anionic phospholipids indicated by the phospholipid monolayer assay may partially explain why polyphemusin I was a relatively good cytoplasmic membrane permeabilizer, while all variants showed significantly decreased ability to depolarize the cytoplasmic membrane of *E. coli.* It is interesting to note that the ability of a peptide to interact with model membranes may correlate with the ability to dissipate the bacterial cytoplasmic membrane potential; however, the lack of cytoplasmic membrane depolarization activity did not correlate with MICs (e.g., as observed for PV5). It appears that all of the peptides can interact well with membranes, however, as suggested previously (*25*), the membrane may not represent the lethal target for all of these peptides. It is evident from the assessment of cell viability alongside the membrane permeabilization assay that cytoplasmic membrane permeabilization by polyphemusin I appears to proceed the death of cells. This is consistent with the observation that other agents able to dissipate the cytoplasmic membrane potential, e.g., carbonyl cyanide *m*-chlorophenyl hydrazone, are actually bacteriostatic rather than bactericidal like these peptides. It is very likely that there might be multiple targets for antimicrobial cationic peptides, and bacterial cell death may not be the result of a single killing mechanism. The decreased membrane activity of the variants also may contribute to the decreased hemolytic activity against red blood cells. The larger effect of these peptides on PG monolayers as compared to CL monolayers is particularly interesting, since a CL molecule has two negative charges, while a PG molecule has only one. This may indicate that electrostatic interactions are not the only driving force for peptide insertion. It is possible that electrostatic interactions play an important role in initial binding of peptides to the monolayer lipid headgroups but that hydrophobic interactions become more important for peptide insertion.

The model structure obtained from the peptide modeling program Insight II and based on the published NMR data of tachyplesin I assumes that polyphemusin I forms the same structure due to its extensive sequence identity and analogous CD spectrum. This model indicates that polyphemusin I is not a strongly amphipathic molecule but rather that the positively charged surface is separated into three blocks by apolar residues (Figure 1, panel B). The three variants were designed so that most of the hydrophobic residues would be clustered to one side, while the majority of the positive charged side chains would be positioned on the other side of the molecule (Figure 1, panel B). Such an amphipathic structure would suggest that these variants were capable of interacting with biological membranes. Indeed all of the peptides were capable of interacting with membranes as demonstrated by tryptophan fluorescence and CD spectrometry. However, to our surprise, none of the variants were strongly capable of permeabilizing the *E. coli* cytoplasmic membrane or of intercalating into phospholipid monolayers as well as the native peptide polyphemusin I. It is interesting to speculate how polyphemusin I insertion would induce the observed increase in membrane permeability. Keeping in mind that the length of a folded polyphemusin I or its variants is apparently insufficient to span the bacterial membrane bilayer, it seems likely that these peptides may interact with a single leaflet of the lipid bilayer, so that the backbone lies parallel to the membrane surface as proposed for other peptides (*40*, *41*). For example, polyphemusin I may interact with the outer leaflet of a lipid bilayer. The two hydrophobic blocks separated by the positively charged residues in polyphemusin I may cause the molecule to deeply partition into the apolar membrane, thereby also immersing the charged surface into fatty acyl chain region so that the highly charged, multiple aromatic residues would then sequester the charges and hydrophobic residues into pockets, thus causing membrane permeabilization by interfering with lipid organization and packing. The variants, however, due to their putative improved amphipathic nature, may reside more superficially in the membrane headgroup−acyl chain interface in a position nearly parallel to the headgroups. This may lead to only mild disturbance of lipid organization and packing thus resulting in reduced activity in membrane permeabilization.

The initial interaction of antimicrobial cationic peptides with Gram-negative bacterial cells involves interaction with the surface LPS, a bulky glycolipid that occupies much of the surface of such bacteria. LPS is a polyanion by virtue of

its possession of multiple phosphate residues and the acidic sugar 2-keto-3-octulosonate in its lipid A-inner core region and is partially neutralized by divalent cations, especially Mg^{2+} ions. Consistent with this, Mg^{2+} ions have been shown to competitively inhibit the action of antimicrobial peptides (*37*). We were able to demonstrate for the first time that peptides actually can insert into a monolayer made entirely from LPS and that the increase in surface pressure was sensitive to antagonism by Mg^{2+} ions. Thus electrostatic interactions must play a major role in the eventual insertion of the peptide into LPS monolayers. All of the peptides had a high affinity for LPS. Interestingly, the peptide with the highest affinity for LPS, PV5 (Table 2), was the most resistant to divalent cation inhibition of insertion into LPS monolayers (Figure 7), the best inhibitor of LPS-induced cytokine production in macrophages (Table 4) and was the most protective in a mouse endotoxic shock model (Table 5). Apparently, like most antimicrobial cationic peptides (*13*), both polyphemusin I and its variants tend to bind to divalent cation binding sites on LPS molecules, competitively displace these divalent cations from their binding sites, and penetrate into the outer membrane. This subsequently causes permeabilization of the outer membrane. Consistent with their high LPS affinity, polyphemusin I and its variants were able to permeabilize the bacterial outer membrane to a similar extent as indicated by their P_{50} values assessed in the NPN uptake assay (Table 2).

Endotoxemia is thought to be a consequence of the effect of monocyte-derived cytokines such as tumor necrosis factor alpha (TNF-α), interleukin 1 (IL-1), and IL-6, which are induced in response to bacterial endotoxin. Although both polyphemusin I and its variants were able to bind strongly to bacterial LPS in vitro and inhibited production of the inflammatory cytokines, TNF-α and IL-6, by LPS-stimulated macrophages (Table 4), all variant peptides showed improved activity relative to polyphemusin I to prevent LPS-induced TNF responses with both a RAW macrophage cell line and galactosamine-sensitized mice. It seems that the structural changes in the polyphemusin I variants improved their ability to provide effective neutralization of the cytokine responses evoked by endotoxin and to block endotoxin shock in an animal model. Similarly, the variants demonstrated superior ability to protect against infections in the animal model, despite their poorer MICs. We studied here the relative ability of peptides to kill bacteria in vitro and in vivo, and there was no obvious formal relationship between these two activities. There are several possible reasons for this. First, it is possible that the protective ability of polyphemusin I was undermined by other (negative) interactions with the host, possibly reflecting the increased in vitro hemolytic activity of this peptide. Second, the peptides may have different stabilities in vivo. Third, protection in animal models may be mediated through mechanisms other than direct bacterial killing by the peptide, including a stimulation of innate immunity or synergy with host factors such as lysozyme (*36*). Regardless of which explanation proves true, these data underscore the necessity to consider the activity of peptides in animal models as part of the design of improved variants.

In summary, our data indicate that increase of amphipathicity of polyphemusin I generally resulted in variants with reduced membranic activity, which may account for decreased toxicity. More significantly, modulation of amphipathicity of polyphemusin I greatly enhanced peptide anti-endotoxin activity, which, to our knowledge, has never been reported before. Since new approaches to the therapy of sepsis and antibiotic-resistant organisms are urgently needed, our findings suggest that the polyphemusin variants have the potential to impact on these syndromes in humans. Further work needs to be done to evaluate the therapeutic potential of these peptides.

REFERENCES

1. Nakamura, T., Furunaka, H., Miyata, T., Tokunaga, F., Muta, T., Iwanaga, S., Niwa, M., Takao, T., and Shimonishi, Y. (1988) *J. Biol. Chem. 263*, 16709−16713.
2. Miyata, T., Tokunaga, F., Yoneya, T., Yoshikawa, K., Iwanaga, S., Niwa, M., Takao, T., and Shimonishi, Y. (1989) *J. Biochem. 106*, 663−668.
3. Masuda, M., Nakashima, H., Ueda, T., Naba, H., Ikoma, R., Otaka, A., Terakawa, Y., Tamamura, H., Ibuka, T., Murakami, T., Koyanagi, Y., Waki, M., Matsumoto, A., Yamamoto, N., Funakoshi, S., and Fujii, N. (1992) *Biochem. Biophys. Res. Commun. 189*, 845−850.
4. Morimoto, M., Mori, H., Otake, T., Ueda, N., Kunita, N., Niwa, M., Murakami, T., and Iwanaga, S. (1991) *Chemotherapy 37*, 206−211.
5. Murakami, T., Niwa, M., Tokunaga, F., Miyata, T., and Iwanaga, S. (1991) *Chemotherapy 37*, 327−334.
6. Yonezawa, A., Kuwahara, J., Fujii, N., and Sugiura, Y. (1992) *Biochemistry 31*, 2998−3004.
7. Kawano, K., Yoneya, T., Miyata, T., Yoshikawa, K., Tokunaga, F., Terada, Y., and Iwanaga, S. (1990) *J. Biol. Chem. 265*, 15365−15367.
8. Park, N. G., Lee, S., Oishi, O. et al. (1992) *Biochemistry 31*, 12241−12247.
9. Tamamura, H., Kuroda, M., Masuda, M., Otaka, A., Funakoshi, S., Nakashima, H., Yamamoto, N., Waki, M., Matsumoto, A., Lancelin, J. M., Kohda, D., Tate, S., Inagaki, F., and Fujii, N. (1993) *Biochim. Biophys. Acta 1163*, 209−216.
10. Tamamura, H., Imai, M., Ishihara, T., Masuda, M., Funakoshi, H., Oyake, H., Murakami, T., Arakaki, R., Nakashima, H., Otaka, A., Ibuka, T., Waki, M., Matsumoto, A., Yamamoto, N., and Fujii, N. (1998) *Bioorg. Med. Chem. 6*, 1033−1041.
11. Arakaki, R., Tamamura, H., Premanathan, M., Kanbara, K., Ramamna, S., Mochizuki, K., Baba, M., Fujii, N., and Nakashima, H. (1999) *J. Virol. 73*, 1719−1723.
12. Katsu, T., Nakao, S., Iwanaga, S. (1993) *Bio. Pharm. Bull. 16*, 178−181.
13. Hancock, R. E. W. (1997). *Lancet 349*, 418−422.
14. Kagan, B. L., Selsted, M. E., Ganz, T., and Lehrer, R. I. (1990) *Proc. Natl. Acad. Sci. U.S.A. 87*, 210−214.
15. Ludtke, S., He, K., Heller, W. T., Harroun, T. A., Yang, L., and Huang, H. W. (1996) *Biochemistry 35*, 13723−13728.
16. Clark, D. (1984) *FEMS Microbiol. Lett. 21*, 189−195.
17. Hooper, D. C., Wolfson, J. S., Ng, E. Y., and Swartz, M. N. (1987) *Am. J. Med. 82* (Suppl. 4A), 12−20.
18. Fields, P. I., Grosman, E. A., and Heffron, F. (1989) *Science 243*, 1059−1062.
19. Hancock, R. E. W., and Carey, A. M. (1979) *J. Bacteriol. 140*, 902−910.
20. Poole, K., Krebes, K., NcNally, C., and Neshat, S. (1993) *J. Bacteriol. 175*, 7363−7372.
21. Moore, R. A., Bates, N. C., and Hancock, R. E. W. (1986) *Antimicrob. Agents Chemother. 29*, 496−500.
22. Merrifield, R. B. (1986) *Science 232*, 341−347.
23. Tam, J. P., Wu, C.-R., Liu, W., and Zhang, J.-W. (1991) *J. Am. Chem. Soc. 113*, 6657−6662.
24. Wu, M., and Hancock, R. E. W. (1999) *J. Biol. Chem. 274*, 29−35.
25. Zhang, L., Benz, R., and Hancock, R. E. W. (1999) *Biochemistry 38*, 8102−8111.

26. Gough, M., Hancock, R. E. W., and Kelly, N. M. (1996) *Infect. Immun. 64*, 4922−4927.
27. Loh, B., Grant, C., and Hancock, R. E. W. (1984) *Antimicrob. Agents Chemother. 26*, 546−551.
28. Sims, P. J., Waggoner, A. S., Wang, C.-H., and Hoffman, J. F. (1974) *Biochemistry 13*, 3315−3330.
29. Mayer, L. D., Nelsestuen, G. L., and Brockman, H. L. (1983) *Biochemistry 22*, 316−321.
30. Eftink, M. R., and Ghiron, C. A. (1976) *J. Phys. Chem. 80*, 486−493.
31. Oshi, D., Yamashita, S., Nishimoto, E., Lee, S., Sugihara, G., and Ohno, M. (1997) *Biochemistry 36*, 4352−4359.
32. Fried, V. A., and Rothfield, L. I. (1978) *Biochim. Biophys. Acta 514*, 69−82.
33. Rao, A. G. (1999) *Arch. Biochem. Biophys. 361*, 127−134.
34. Chang, C. T., Wu, C. S., and Yang, J. T. (1978) *Anal. Biochem. 91*, 13−17.
35. Hristova, K., Selsted, M. E., and White, S. H. (1997) *J. Biol. Chem. 272*, 24224−24233.
36. Scott, M., Yan, H., and Hancock, R. E. W. (1999) *Infect. Immun. 67*, 2005−2009.
37. Falla T. J., Karunaratne, D. N., and Hancock, R. E. W. (1996) *J. Biol. Chem. 271*, 19298−19303.
38. Lehrer, R. I., Barton, A., Daher, K. A., Harwig, S. S. L., Ganz, T., and Selsted, M. E. (1989) *J. Clin. Invest. 84*, 553−561.
39. Wu M. Maier, E., Benz, R., and Hancock, R. E. W. (1999). *Biochemistry 38*, 7235−7242.
40. Bechinger, B., Zasloff, M., and Opella, S. J. (1993) *Protein Sci. 2*, 2077−2084.
41. Hwang, P. M., Zhou, N., mShan, X., Arrowsmith, C. H., and Vogel, H. J. (1998) *Biochemistry 37*, 4288−4298.

BI0011173